ACS Catalysis

pubs.acs.org/acscatalysis Letter

Gas-Phase Ethylene Polymerization by Single-Site Cr Centers in a Metal–Organic Framework

Hoyoung D. Park, Robert J. Comito, Zhenwei Wu, Guanghui Zhang, Nathan Ricke, Chenyue Sun, Troy Van Voorhis, Jeffrey T. Miller, Yuriy Román-Leshkov,* and Mircea Dincă*

Cite This: *ACS Catal.* 2020, 10, 3864–3870 Read Online

ACCESS | Metrics & More | Article Recommendations | Supporting Information

ABSTRACT: We report a systematic study on the gas-phase polymerization of ethylene by a metal–organic framework (MOF) catalyst. Cr^{3+}-exchanged MFU-4*l* (Cr(III)-MFU-4*l*, MFU-4*l* = $Zn_5Cl_4(BTDD)_3$, H_2BTDD = bis(1*H*-1,2,3,-triazolo[4,5-*b*],[4′,5′-*i*])dibenzo[1,4]dioxin)) serves as an exemplary system to demonstrate prereaction treatment with alkylaluminum species as a simple method to isolate an active MOF catalyst for liquid-free polymerization of ethylene. $AlMe_3$-treated Cr(III)-MFU-4*l* subjected to 40 bar of ethylene exhibits a polymerization activity of 52 000 $mol_{Ethylene} \cdot mol_{Cr}^{-1} \cdot h^{-1}$, an order of magnitude higher than that observed in a slurry-phase reaction with Cr(III)-MFU-4*l* and excess alkylaluminum species. Furthermore, product polyethylene exhibits a low polydispersity index of 1.36 and a free-flowing granular morphology favorable for industrial processing, highlighting the advantages conferred by the single-site MOF catalysts in gas-phase ethylene polymerization.

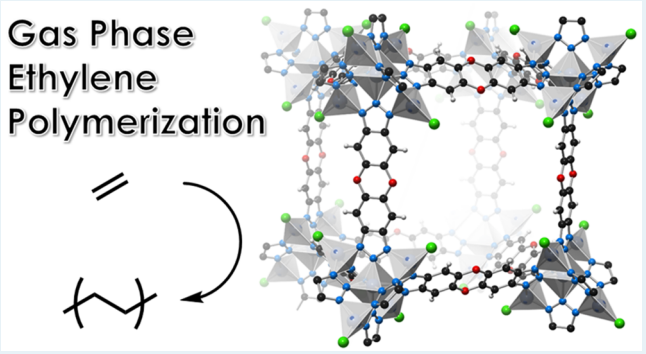

KEYWORDS: *metal–organic framework, heterogeneous catalysis, single-site catalyst, polyethylene, gas-phase polymerization*

The advent of the gas-phase ethylene polymerization process, epitomized by the commercialization of the UNIPOL process by Union Carbide in 1968, transformed the modern production of polyethylene plastics.[1] A key to its commercial success lies in the use of inexpensive fluidized bed reactors devoid of energy-intensive liquid-phase operations, resulting in a nearly 30% reduction in reactor construction and operation costs over conventional liquid-phase processes.[2] Moreover, gas-phase processes are not restricted by the inherent solubility and viscosity constraints in liquid-phase processes that limit the range of producible polyethylenes and often cause complications with polymer agglomeration and reactor fouling.[3] To exploit these advantages, decades of research has been focused on developing heterogeneous polymerization catalysts that can reproduce the high degree of reactivity control afforded by the molecular single-site catalysts.[4,5] This effort has become increasingly relevant given the growing demand for advanced polyolefins with precise polymer microstructures and molecular-weight profiles for tailored material properties.[6] Such stringent requirements can be met, for instance, by a concomitant use of multiple single-site catalysts in a single process to produce polyethylenes with the desired multimodal molecular weight distributions.[7,8] Thus far, the synthesis of heterogeneous polymerization catalysts has largely involved chemically immobilizing the active metal species onto porous supports to achieve high dispersion of surface species available for gas-phase reaction.[9−11] However, lack of precise molecular control over the immobilization process leads to variability in the final structure of the supported species, which ultimately results in numerous active-site local environments with vastly differing polymerization rates.[12] Furthermore, a large number of bound sites often become inaccessible to the substrate because of multinuclear agglomeration upon immobilization.[13] These challenges are manifested in the high polydispersity of the polymer products and underutilization of the active component for various heterogeneous ethylene polymerization catalysts.[14,15] For example, Phillips chromium-oxide catalysts that currently produce the majority of commercial high-density polyethylenes (HDPE) are known to have only ∼10% of their chromium centers that are active in the production of polyethylenes with polydispersity indices (PDI = M_W/M_N, M_W = weight-averaged molecular weight, M_N = number-averaged molecular weight) varying from 4.0 to 100.[14,16]

Received: August 2, 2019
Revised: February 24, 2020
Published: March 3, 2020

Unlike the active sites in most conventional solid catalysts, the metal sites in the inorganic nodes of metal−organic frameworks (MOFs) exhibit remarkable structural uniformity because of the intrinsic crystalline nature of the framework.[17−19] Furthermore, numerous coordination geometries afforded by the ligating organic linkers provide the node metals with unusual electronic environments that can promote the desired interactions with the substrate.[20−22] Combined with the site-isolated nature of these metal ions that are readily accessible through a porous network, the coordinatively unsaturated metal sites of MOFs offer opportunities for single-site catalysis uncommon to traditional supported catalysts.[23−26] Accordingly, there have been efforts to utilize these node metal centers as active sites for ethylene polymerization.[27,28] However, MOF catalysts for this process have required alkylaluminum cocatalysts such that studies have been limited exclusively to slurry-phase reactions. The same holds true, for instance, for our previously reported olefin polymerization catalysts based on cation-exchanged MFU-4*l* (MFU-4*l* = $Zn_5Cl_4(BTDD)_3$, H_2BTDD = bis(1*H*-1,2,3-triazolo[4,5-*b*],[4′,5′-*i*])dibenzo[1,4]dioxin))[25,29,30] that feature a wide variety of active metal cations (Ti, V, Cr, or Co) replacing the peripheral tetrahedral Zn^{2+} ions of the parent framework (Figure 1).[31−34] Whereas these metals are placed in a tripodal coordination environment reminiscent of those found in molecular scorpionate complexes and exhibit analogous olefin polymerization activity,[35,36] the MOF catalysts are completely inactive in the absence of alkylaluminum cocatalysts. This cocatalyst dependence and consequent restriction to liquid-phase operations have limited the utility of these and other MOF catalysts, since gas-phase ethylene polymerization is the specific application for which the single-site activity and porosity of MOF catalysts can best be leveraged.

Here, we report gas-phase polymerization of ethylene by Cr^{3+}-exchanged MFU-4*l* (Cr(III)-MFU-4*l*, **1**) pretreated with $AlMe_3$. Despite the absence of excess aluminum cocatalysts during catalysis tests, the MOF catalyst shows activity for gas-phase ethylene polymerization that is nearly 10-fold higher than the slurry-phase activity of **1**, which notably requires excess alkylaluminum under identical pressures and temperatures. The catalyst shows no appreciable deactivation for at least 24 h and produces dry beads of HDPE. Product polyethylene displays a low PDI of 1.36, underscoring the high degree of molecular weight control provided by our single-site MOF catalyst.

To probe the possibility of realizing gas-phase polymerization with these catalysts, we prepared **1** and Cr^{2+} exchanged MFU-4*l* (Cr(II)-MFU-4*l*, **2**) as previously reported, by soaking MFU-4*l* in *N*,*N*-dimethylformamide (DMF) solutions of $CrCl_3$ or $CrCl_2$.[32] For **1**, a near-complete exchange of the tetrahedral Zn^{2+} in MFU-4*l* for chromium cations was achieved using 20 equiv of $CrCl_3$ and a catalytic amount of $CrCl_2$ at room temperature (Figures 1 and S7−S9, and Table S3). In contrast, a lower extent of cation exchange at Cr_{mol}:Zn_{mol} = 2.45:2.55 was obtained with just Cr^{2+} in forming **2** (Table S3). For **1**, DMF in the as-synthesized material can be removed by first exchanging with methanol and drying the recovered solids under dynamic vacuum at 150 °C (Figure S10). Notably, a distinct color change from forest green to a bright yellow upon solvent removal qualitatively suggests a change in the primary coordination sphere of the exchanged chromium centers.

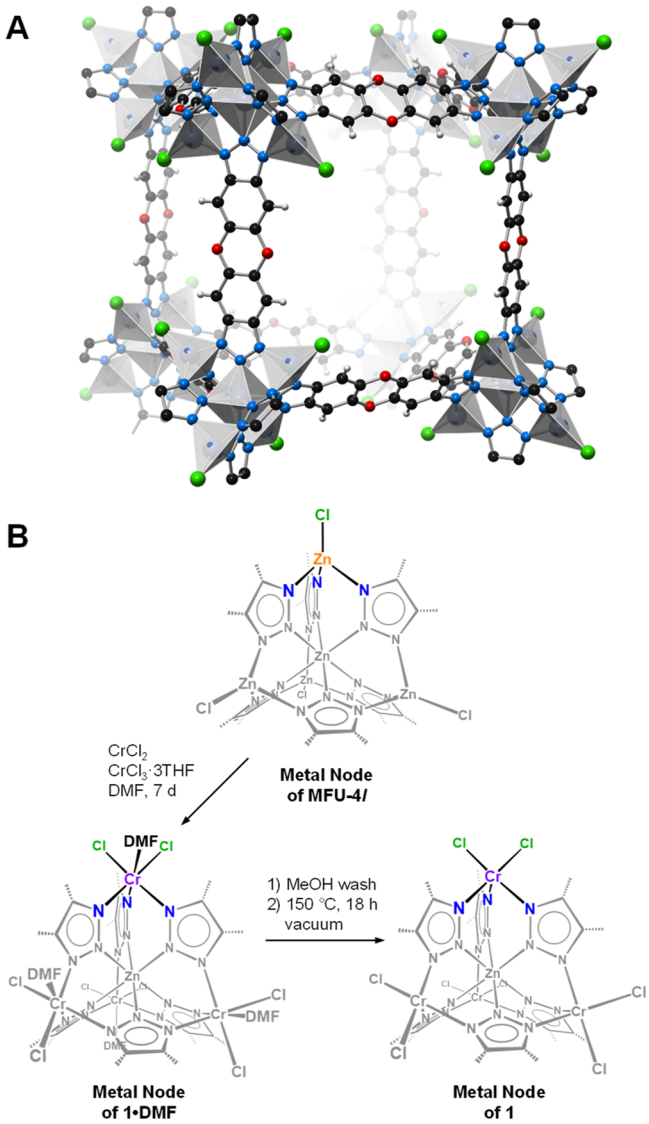

Figure 1. (A) Crystal structure of MFU-4*l*. (B) Illustration of the inorganic nodes of MFU-4*l* and their transformation to those of Cr^{3+}-exchanged MFU-4*l* (**1**) via cation exchange and desolvation.

Chromium K-edge X-ray absorption spectroscopy (XAS) provided important information on the oxidation state and the coordination environment of chromium in **1** and **2**. For comparison, a batch of Cr(III)-MFU-4*l* coordinated with DMF was prepared without performing the methanol exchange (**1**·DMF). We also analyzed $Tp_2Cr(II)$, $TpCr(III)Cl_2$·py, $Tp_2Cr(III)PF_6$, and $Tpm^*Cr(III)Cl_3$ (Tp^- = tris(pyrazolyl)borate, py = pyridine, and Tpm* = tris(3,5-dimethylpyrazolyl)methane) as standards for Cr(II) and Cr(III) in the node of MFU-4*l*, having found analogous scorpionate complexes to be reliable XAS standards for nickel-, cobalt-, and vanadium-exchanged MFU-4*l*.[33,34,37] X-ray absorption near edge spectroscopy (XANES) analysis indicated a Cr(III) oxidation state for **1** and a Cr(II) oxidation state for **2** (Figure 2A,B); the edge energies of **1**·DMF and desolvated **1**, defined as the maximum of the first derivative of the XANES curve, were indistinguishable at 5999.5 eV and fit among those of our Cr(III) standards, while that of **2** at 5996.1 eV was lower and much closer to the edge energies of the Cr(II) standards. The existence of a small percentage of Cr(III) species in **2**, however, cannot be ruled

https://dx.doi.org/10.1021/acscatal.9b03282
ACS Catal. 2020, 10, 3864−3870

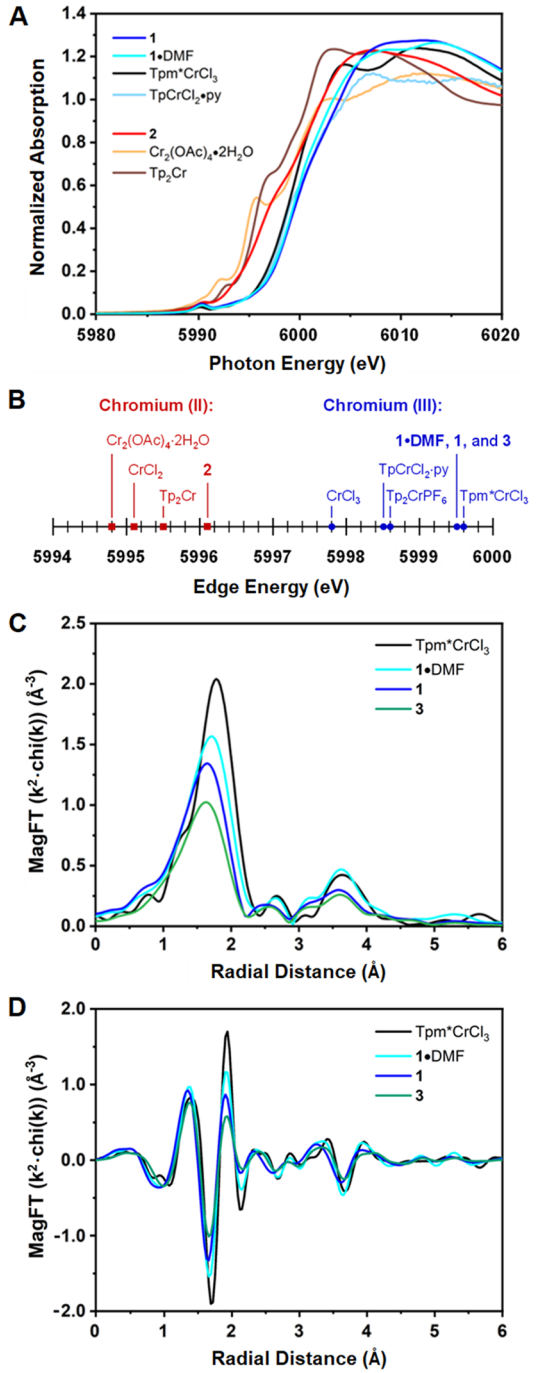

Figure 2. (A) Chromium K-edge XANES spectra of **1**·DMF, **1**, **2**, and relevant standards (Tp^- = tris(pyrazolyl)borate, Tpm* = tris(3,5-dimethylpyrazolyl)methane, and py = pyridine). (B) XANES edge energies of **1**·DMF, **1**, **2**, **3**, and relevant standards. (C) The magnitude of the Fourier-transformed k^2-weighted EXAFS spectra of **1**·DMF, **1**, **3**, and Tpm*$CrCl_3$. (D) The imaginary part of the Fourier-transformed k^2-weighted EXAFS spectra of **1**·DMF, **1**, **3**, and Tpm*$CrCl_3$.

out. The pre-edge peaks that originate from the Cr 1s−3d transition in **1**, **1**·DMF, and **2** all had relatively low intensities similar to those of the pseudo-octahedrally coordinated chromium standards. This ruled out a pseudotetrahedral chromium coordination geometry for **1**, **1**·DMF, and **2**, as such an arrangement is expected to produce pre-edge features with much higher intensity (Figure S11).[38] Going from Tpm*$CrCl_3$ to **1**·DMF and to **1**, the main Cr(III) pre-edge peak showed an increase in peak intensity, indicating increased deviation away from the centrosymmetry around the Cr(III) center. This is consistent with the expected differences in the first coordination sphere of Cr(III) in Tpm*$CrCl_3$, **1**·DMF, and **1**, where a chlorine ligand in Tpm*$CrCl_3$ would be replaced by an oxygen in **1**·DMF and would be absent in **1** (Figure 1B).

The extended X-ray absorption fine structure (EXAFS) region of the XAS spectrum of dried **1** showed a first-shell peak that was similar in shape and position but reduced in intensity to those of **1**·DMF and Tpm*$CrCl_3$ in both the magnitude and imaginary parts of the Fourier tranform of EXAFS (Figure 2C,D). This suggests similar coordination environments but a reduced coordination number in **1**, further evidence for coordinative unsaturation in **1**. In addition, features from Cr−Cr bonding were clearly absent, confirming the singly dispersed nature of the Cr active sites. We next performed first-shell fits of the EXAFS data from **1** and **1**·DMF (Figures S12), and we compared them to the EXAFS data from Tp_2CrPF_6 and Tpm*$CrCl_3$ standards as well as to the computational models of **1** and **1**·DMF by density functional theory (DFT) (Section S4). This analysis considered multiple models where the coordination numbers were integers matching the possible Cr coordination structures, while all other variables were optimized during the fitting process. This resulted in primary coordination spheres consisting of 3 Cr−N and 2 Cr−Cl bonds for **1**, and 4 Cr−N[39] and 2 Cr−Cl bonds for **1**·DMF (Table 1). Modeling of other coordination

Table 1. Results of the EXAFS and DFT Analyses[a]

sample	scattering pair	CN[b]	bond length (Å)	S_0^2	ΔE_0 (eV)	σ^2 (Å^2)
1·DMF	Cr−N/O[39]	4	2.03	0.69	−2.9	0.004
	Cr−Cl	2	2.27			0.002
1	Cr−N	3	1.99	0.69	−5.4	0.002
	Cr−Cl	2	2.26			0.002
DFT-**1**·DMF	Cr−N/O[39]	4	2.058	-	-	-
	Cr−Cl	2	2.351	-	-	-
DFT-**1**	Cr−N	3	2.032	-	-	-
	Cr−Cl	2	2.290	-	-	-
Tp_2CrPF_6	Cr−N	6	2.02	0.65	−2.3	0.002
Tpm*$CrCl_3$	Cr−Cl	3	2.29	0.69	−1.3	0.002

[a]The average error in the EXAFS-derived bond lengths is 0.02 Å, in ΔE_0 is 2.3 eV, and in σ^2 is 0.001 Å^2. [b]CN = coordination number (CN was held constant during the EXAFS fitting).

numbers and geometries resulted in quantitatively worse fits, while the resulting bond lengths agreed well with those obtained by DFT and EXAFS analyses of the standards. Furthermore, our DFT models showed a pseudooctahedral coordination in **1**·DMF that converts to a pseudosquare pyramidal or monovacant octahedral geometry for **1** upon removal of coordinated DMF (Section S4). Indeed, these results are highly consistent with the reported structure of other coordinatively unsaturated chromium tris(pyrazolyl)-borate complexes.[40] EXAFS fits were not obtained for **2**, which is due perhaps to the differing degree of solvation around individual Cr(II) centers. The XAS data support a scenario wherein cation exchange initially affords an octahedral Cr(III) center in **1**·DMF bearing one DMF molecule (Figure 1B). Subsequent solvent exchange and drying results in a five-

https://dx.doi.org/10.1021/acscatal.9b03282
ACS Catal. 2020, 10, 3864−3870

coordinate, pseudosquare pyramidal Cr(III) in **1**, with one open coordination site.

With the presumed structure of **1** in hand, we next sought ways to convert it to an active catalyst for gas-phase ethylene polymerization. Although alkylchromiums are often invoked as the active species for chromium-based ethylene polymerization, their high reactivity demands rigorous site isolation to be observed experimentally.[12,40] Consequently, active chromium catalysts are conventionally generated *in situ* from precatalysts by adding excess alkylaluminum cocatalysts to the reaction medium or by subjecting the supported precatalysts to ethylene atmosphere at elevated temperatures. Given the site-isolated nature of the node metals in MOFs, we surmised that *ex situ* activation of **1** with alkylaluminums could provide a stable and isolable Cr(III) alkyl. Such a species suspended within a porous scaffold would then be accessible to incoming ethylene molecules for gas-phase polymerization. To this end, **1** was treated with 0.2 M of $AlMe_3$ in hexane and vacuum-dried after filtration. The dry, $AlMe_3$-treated Cr(III)-MFU-4*l* (**3**) is crystalline and porous, as confirmed by powder X-ray diffraction (PXRD) and N_2 sorption analyses (Figures S7 and S8). Inductively coupled plasma-mass spectrometry (ICP-MS) analysis revealed a molar Cr:Al ratio of 1:1.8 for **3**, indicating some retention of aluminum species within the framework (Table S3). Chromium K-edge XANES spectrum of **3** (Figure S13) showed an edge energy at 5999.5 eV and a main pre-edge peak at 5990.5 eV that were unchanged from those of **1** and **1**·DMF, suggesting that the majority of chromium centers remained Cr(III) following treatment with $AlMe_3$. The leading edge shifted to lower energy, which was consistent with the proposed coordination of electron-rich alkyl groups on the chromium centers, though the possibility of partial reduction into Cr(II) cannot be excluded.[41−43] The EXAFS region of **3** is remarkably similar to that of **1**, with the only major difference that the first shell peak displays a diminished scattering intensity (Figure 2C). The reduced intensity is consistent with the presumed alkylation from Cr(III)−Cl to Cr(III)−CH_3 while maintaining the node structure around the chromium centers.

The gas-phase ethylene polymerization activity of **3** was probed by subjecting it to semibatch reactions under constant ethylene pressure in the complete absence of solvent or additional cocatalyst. Reactions were first conducted without external temperature control to compare the polymerization activity in the gas-phase against those of slurry-phase reactions reported previously. Notably, static pressurization of 2.0 mg of **3** at room temperature with 40 bar of ethylene for 1 h yielded 7.06 g polyethylene as free-flowing white granules (Figures 3 and S14). This activity corresponds to a turnover frequency of 52 000 $mol_{Ethylene}·mol_{Cr}^{-1}·h^{-1}$, more than an order of magnitude higher than that observed when **1** was subjected to analogous slurry-phase reactions in the presence of excess $AlMe_3$ (Table 2). To account for this difference in activity, we propose that solvation and subsequent diffusion of ethylene to the active sites of the catalyst constitute an additional kinetic barrier under slurry-phase conditions. Neither $AlMe_3$-treated MFU-4*l* nor pristine **1** polymerized ethylene under these conditions, confirming that both the cation-exchanged chromium centers in **1** and their subsequent treatment with $AlMe_3$ are required for catalysis (Table 2).

On the basis of differential scanning calorimetry characterization, we assign the polyethylene product from a gas-phase reaction as linear HDPE; its second-scan melting at 130 °C and crystallinity of 66% being consistent with HDPE of high molecular weight (Figure S15).[44] This result is consistent not only with what we had observed previously for slurry-phase polymerization with **1** but also with the lack of chain walking in early transition metal catalysts.[45,46] Further analysis with high-temperature gel permeation chromatography revealed a number-averaged molecular weight (M_N) of 298 kDa and a remarkably low PDI of 1.36 for the polymer product (Figure S16). This exceptionally low PDI value demonstrates the structural monodispersity of the active sites in our catalyst and also suggests facile gas-phase diffusion of ethylene to the active sites. Indeed, mass transport limitations are known to increase PDI through inhomogeneous local ethylene concentions.[47−49] It is also noteworthy that the polyethylene product is directly obtained in the form of free-flowing granular beads, the favored morphology for industrial processing of polyethylenes (Figure 3).[13]

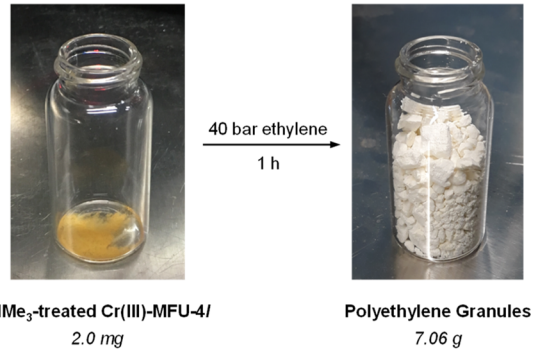

Figure 3. $AlMe_3$-treated Cr(III)-MFU-4*l* (**3**) before and after a gas-phase ethylene polymerization reaction (Table 2, entry 1).

Expectedly, when the gas-phase ethylene polymerization reaction with **3** is run without external temperature control, the temperature of the reactor increases spontaneously during the course of the reaction (Figure S18). We ascribe this exotherm to the high heat of reaction from ethylene polymerization (ΔH^0_{rxn} = 93.6 kJ·mol^{-1}) that was retained in our batch reactor system.[3] This exothermic behavior, combined with the possible intrapore condensation of ethylene at elevated pressures,[50,51] caused the linear dependence of polymerization activity on ethylene pressure to deviate at higher pressures, where higher activities were obtained (Figure S18). To account for the exothermicity, we conducted a control reaction where **1** and excess $AlMe_3$ in toluene were subjected to 40 bar of ethylene for 1 h at 35 °C, the average temperature measured from a gas-phase reaction with **3** (Table 2, entry 5). Surprisingly, the liquid-phase reaction with **1** and $AlMe_3$ at elevated temperature resulted in activity even lower than that of the identical reaction conducted without heating. We attribute this behavior to the thermally accelerated deactivation of **1** in the presence of excess $AlMe_3$ and solvent: under these conditions, alkylaluminums are known to exchange the active sites in the nodes of MFU-4*l* and cause subsequent reduction, aggregation, and formation of transition metal nanoparticles.[52] Importantly, these deactivation pathways are inaccessible to **3**, whose catalytic activity does not require liquid medium or additional alkylaluminum. Indeed, not only does **3** retain its activity despite autogenous heating, but its activity persists and no appreciable deactivation is observed even for prolonged reaction times of 24 h (Figure 4).

https://dx.doi.org/10.1021/acscatal.9b03282
ACS Catal. 2020, 10, 3864−3870

Table 2. Results of Ethylene Polymerization Reactions[a]

entry	catalyst	cocatalyst	solvent	$P_{Ethylene}$ (bar)	t (h)	TOF[b] ($mol_{Ethylene} \cdot mol_{Cr}^{-1} \cdot h^{-1}$)	T_m[c] (°C)	X_C[c] (%)	PDI[d]	M_N[e] (kDa)
1	$AlMe_3$-treated Cr(III)-MFU-4*l*	none	none	40	1	52 000	130	66	1.36	298
2	Cr(III)-MFU-4*l*	$AlMe_3$[f]	toluene	40	1	4500	130	66	1.42	331
3	Cr(III)-MFU-4*l*	none	none	40	1	0	-	-	-	-
4	$AlMe_3$-treated MFU-4*l*	none	none	40	1	0	-	-	-	-
5[g]	Cr(III)-MFU-4*l*	$AlMe_3$[f]	toluene	40	1	3800	130	64	1.48	297

[a]Unless otherwise noted, reactions were conducted at room temperature without external temperature control. [b]TOF = turnover frequency. [c]Melting peak (T_m) and second scan percent crystallinity (X_C) as evaluated by differential scanning calorimetry. [d]PDI = polydispersity index [e]M_N = number-averaged molecular weight. [f]100 mol equiv of $AlMe_3$ to the ICP-MS-derived moles of chromium in Cr(III)-MFU-4*l*. [g]Reaction conducted at 35 °C.

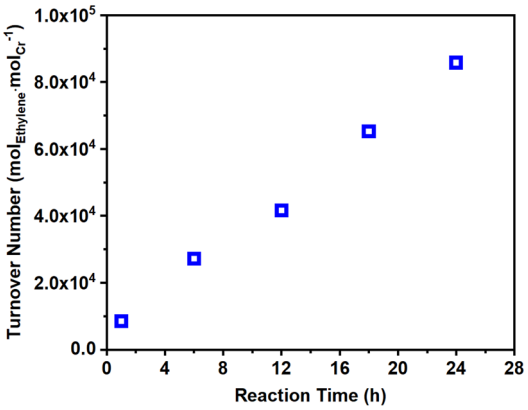

Figure 4. Gas-phase ethylene polymerization with $AlMe_3$-treated Cr(III)-MFU-4*l* (**3**). Reaction conditions: 2.0 mg catalyst, 10 bar ethylene, and room temperature without external temperature control.

In summary, we show for the first time that MOFs are capable catalysts for gas-phase ethylene polymerization, with activity and lifetime surpassing those of the slurry-phase process. Isolation of Cr-alkyl species prior to catalytic tests affords active MOFs that do not require solvent or the presence of excess *in situ* alkylaluminum cocatalyst. HDPE produced by this catalyst in the gas-phase presents as free-flowing granules with exceptionally low polydispersity. We attribute this favorable performance of the catalyst to the site accessibility and structural uniformity unique to the isolated single sites of the MOF platform. We believe these intrinsic structural advantages could be further utilized to develop improved MOF catalysts for the commercially important gas-phase ethylene polymerization reaction.

■ ASSOCIATED CONTENT

Supporting Information

The Supporting Information is available free of charge at https://pubs.acs.org/doi/10.1021/acscatal.9b03282.

Experimental information and supplementary data (PDF)

■ AUTHOR INFORMATION

Corresponding Authors

Mircea Dincă − *Department of Chemistry, Massachusetts Institute of Technology, Cambridge, Massachusetts 02139, United States;* orcid.org/0000-0002-1262-1264; Email: mdinca@mit.edu

Yuriy Román-Leshkov − *Department of Chemical Engineering, Massachusetts Institute of Technology, Cambridge, Massachusetts 02139, United States;* orcid.org/0000-0002-0025-4233; Email: yroman@mit.edu

Authors

Hoyoung D. Park − *Department of Chemical Engineering, Massachusetts Institute of Technology, Cambridge, Massachusetts 02139, United States;* orcid.org/0000-0001-6031-2338

Robert J. Comito − *Department of Chemistry, University of Houston, Houston, Texas 77004, United States;* orcid.org/0000-0003-1298-2876

Zhenwei Wu − *Davidson School of Chemical Engineering, Purdue University, West Lafayette, Indiana 47907, United States;* orcid.org/0000-0003-0400-9427

Guanghui Zhang − *School of Chemical Engineering, Dalian University of Technology, Dalian, Liaoning Province 116024, China;* orcid.org/0000-0002-5854-6909

Nathan Ricke − *Department of Chemistry, Massachusetts Institute of Technology, Cambridge, Massachusetts 02139, United States*

Chenyue Sun − *Department of Chemistry, Massachusetts Institute of Technology, Cambridge, Massachusetts 02139, United States*

Troy Van Voorhis − *Department of Chemistry, Massachusetts Institute of Technology, Cambridge, Massachusetts 02139, United States;* orcid.org/0000-0001-7111-0176

Jeffrey T. Miller − *Davidson School of Chemical Engineering, Purdue University, West Lafayette, Indiana 47907, United States;* orcid.org/0000-0002-6269-0620

Complete contact information is available at: https://pubs.acs.org/10.1021/acscatal.9b03282

Notes

The authors declare no competing financial interest.

Safety note: Due to the possibility of a thermal explosion as a result of uncontrolled polymerizations, the reactions in this study were conducted in a well-ventilated hood with a batch reactor that was equipped with appropriate check valves, flashback arrestors, and a pressure relief valve.

■ ACKNOWLEDGMENTS

H.D.P. gratefully acknowledges the Samsung Foundation for support through the Samsung Scholarship program. Y.R.-L. thanks the Department of Energy for funding through the Office of Basic Energy Sciences (DE-SC0016214). Studies of small molecule reactivity in MOFs were supported by a CAREER grant from the National Science Foundation to M.D. (DMR-1452612). Z.W., G.Z., J.T.M. are supported in part by the National Science Foundation under Cooperative Agree-

ment No. EEC-1647722. Any opinions, finding, and conclusions or recommendations expressed in this material are those of the authors and do not necessarily reflect the views of the National Science Foundation. Use of the Advanced Photon Source was supported by the U.S. Department of Energy, Office of Basic Energy Sciences, under contract no. DE-AC02-06CH11357. MRCAT operations, beamline 10-ID, are supported by the Department of Energy and the MRCAT member institutions.

REFERENCES

(1) Karol, F. J. Catalysis and the UNIPOL® Process in the 1990's. *Macromol. Symp.* **1995**, *89*, 563−575.
(2) Xie, T.; McAuley, K. B.; Hsu, J. C. C.; Bacon, D. W. Gas Phase Ethylene Polymerization: Production Processes, Polymer Properties, and Reactor Modeling. *Ind. Eng. Chem. Res.* **1994**, *33*, 449−479.
(3) Whiteley, K. S. Polyethylene. in *Ullmann's Encyclopedia of Industrial Chemistry*; Elvers, B., Ed.; Wiley-VCH: Weinheim, 2012; Vol. *29*, pp 1−38.
(4) Hlatky, G. G. Heterogeneous Single-Site Catalysts for Olefin Polymerization. *Chem. Rev.* **2000**, *100*, 1347−1376.
(5) Harrison, D.; Coulter, I. M.; Wang, S.; Nistala, S.; Kuntz, B. A.; Pigeon, M.; Tian, J.; Collins, S. Olefin Polymerization Using Supported Metallocene Catalysts: Development of High Activity Catalysts for Use in Slurry and Gas Phase Ethylene Polymerizations. *J. Mol. Catal. A: Chem.* **1998**, *128*, 65−77.
(6) Soares, J. B. P.; McKenna, T. F. L. *Polyolefin Reaction Engineering*; Wiley-VCH: Weinheim, 2012.
(7) Stürzel, M.; Mihan, S.; Mülhaupt, R. From Multisite Polymerization Catalysis to Sustainable Materials and All-Polyolefin Composites. *Chem. Rev.* **2016**, *116*, 1398−1433.
(8) Albunia, A. R.; Prades, F.; Jeremic, D. *Multimodal Polymers with Supported Catalysts: Design and Production*; Springer Nature Switzerland AG: Cham, 2012.
(9) Stalzer, M. M.; Delferro, M.; Marks, T. J. Supported Single-Site Organometallic Catalysts for the Synthesis of High-Performance Polyolefins. *Catal. Lett.* **2015**, *145*, 3−14.
(10) Kumkaew, P.; Wanke, S. E.; Praserthdam, P.; Danumah, C.; Kaliaguine, S. Gas-Phase Ethylene Polymerization Using Zirconocene Supported on Mesoporous Molecular Sieves. *J. Appl. Polym. Sci.* **2003**, *87*, 1161−1177.
(11) Kim, S. H.; Somorjai, G. A. Surface Science of Single-Site Heterogeneous Olefin Polymerization Catalysts. *Proc. Natl. Acad. Sci. U. S. A.* **2006**, *103*, 15289−15294.
(12) Copéret, C.; Allouche, F.; Chan, K. W.; Conley, M. P.; Delley, M. F.; Fedorov, A.; Moroz, I. B.; Mougel, V.; Pucino, M.; Searles, K.; Yamamoto, K.; Zhizhko, P. A. Bridging the Gap Between Industrial and Well-Defined Supported Catalysts. *Angew. Chem., Int. Ed.* **2018**, *57*, 6398−6440.
(13) Severn, J. R.; Chadwick, J. C.; Duchateau, R.; Friederichs, N. "Bound but Not Gagged" - Immobilizing Single-Site α-Olefin Polymerization Catalysts. *Chem. Rev.* **2005**, *105*, 4073−4147.
(14) Copéret, C.; Comas-Vives, A.; Conley, M. P.; Estes, D. P.; Fedorov, A.; Mougel, V.; Nagae, H.; Núnez-Zarur, F.; Zhizhko, P. A. Surface Organometallic and Coordination Chemistry toward Single-Site Heterogeneous Catalysts: Strategies, Methods, Structures, and Activities. *Chem. Rev.* **2016**, *116*, 323−421.
(15) Severn, J. R.; Chadwick, J. C. Immobilisation of Homogeneous Olefin Polymerisation Catalysts. *Factors Influencing Activity and Stability. Dalt. Trans.* **2013**, *42*, 8979−8987.
(16) McDaniel, M. P. A Review of the Phillips Supported Chromium Catalyst and Its Commercial Use for Ethylene Polymerization. In *Adv. Catal.*; Gates, B. C., Knözinger, H., Eds.; Elsevier Inc.: Oxford, 2010; Vol. *53*; pp 123−606.
(17) Yaghi, O. M.; Kalmutzki, M. J.; Diercks, C. S. *Introduction to Reticular Chemistry*; Wiley-VCH: Weinheim, 2019.
(18) Song, Y.; Li, Z.; Ji, P.; Kaufmann, M.; Feng, X.; Chen, J. S.; Wang, C.; Lin, W. Metal−Organic Framework Nodes Support Single-Site Nickel(II) Hydride Catalysts for the Hydrogenolysis of Aryl Ethers. *ACS Catal.* **2019**, *9*, 1578−1583.
(19) Otake, K.; Ye, J.; Mandal, M.; Islamoglu, T.; Buru, C. T.; Hupp, J. T.; Delferro, M.; Truhlar, D. G.; Cramer, C. J.; Farha, O. K. Enhanced Activity of Heterogeneous Pd(II) Catalysts on Acid-Functionalized Metal−Organic Frameworks. *ACS Catal.* **2019**, *9*, 5383−5390.
(20) Park, H. D.; Dincă, M.; Román-Leshkov, Y. Continuous-Flow Production of Succinic Anhydrides via Catalytic β-Lactone Carbonylation by $Co(CO)_4$⊂Cr-MIL-101. *J. Am. Chem. Soc.* **2018**, *140*, 10669−10672.
(21) Yuan, S.; Qin, J.; Xu, H.; Su, J.; Rossi, D.; Chen, Y.; Zhang, L.; Lollar, C.; Wang, Q.; Jiang, H.; Son, D. H.; Xu, H.; Huang, Z.; Zou, X.; Zhou, H. $[Ti_8Zr_2O_{12}(COO)_{16}]$ Cluster: An Ideal Inorganic Building Unit for Photoactive Metal−Organic Frameworks. *ACS Cent. Sci.* **2018**, *4*, 105−111.
(22) Ji, P.; Drake, T.; Murakami, A.; Oliveres, P.; Skone, J. H.; Lin, W. Tuning Lewis Acidity of Metal−Organic Frameworks via Perfluorination of Bridging Ligands: Spectroscopic, Theoretical, and Catalytic Studies. *J. Am. Chem. Soc.* **2018**, *140*, 10553−10561.
(23) Kalmutzki, M. J.; Hanikel, N.; Yaghi, O. M. Secondary Building Units as the Turning Point in the Development of the Reticular Chemistry of MOFs. *Sci. Adv.* **2018**, *4*, eaat9180.
(24) Vitillo, J. G.; Bhan, A.; Cramer, C. J.; Lu, C. C.; Gagliardi, L. Quantum Chemical Characterization of Structural Single Fe(II) Sites in MIL-Type Metal−Organic Frameworks for the Oxidation of Methane to Methanol and Ethane to Ethanol. *ACS Catal.* **2019**, *9*, 2870−2879.
(25) Denysenko, D.; Jelic, J.; Reuter, K.; Volkmer, D. Postsynthetic Metal and Ligand Exchange in MFU-4*l*: A Screening Approach toward Functional Metal−Organic Frameworks Comprising Single-Site Active Centers. *Chem. - Eur. J.* **2015**, *21*, 8188−8199.
(26) Park, H. D.; Dincă, M.; Román-Leshkov, Y. Heterogeneous Epoxide Carbonylation by Cooperative Ion-Pair Catalysis in Co-$(CO)_4^-$-Incorporated Cr-MIL-101. *ACS Cent. Sci.* **2017**, *3*, 444−448.
(27) Rivera-Torrente, M.; Pletcher, P. D.; Jongkind, M. K.; Nikolopoulos, N.; Weckhuysen, B. M. Ethylene Polymerization Over Metal−Organic Framework Crystallites and the Influence of Linkers on Their Fracturing Process. *ACS Catal.* **2019**, *9*, 3059−3069.
(28) Ji, P.; Solomon, J. B.; Lin, Z.; Johnson, A.; Jordan, R. F.; Lin, W. Transformation of Metal−Organic Framework Secondary Building Units into Hexanuclear Zr−Alkyl Catalysts for Ethylene Polymerization. *J. Am. Chem. Soc.* **2017**, *139*, 11325−11328.
(29) Denysenko, D.; Grzywa, M.; Jelic, J.; Reuter, K.; Volkmer, D. Scorpionate-Type Coordination in MFU-4*l* Metal−Organic Frameworks: Small-Molecule Binding and Activation upon the Thermally Activated Formation of Open Metal Sites. *Angew. Chem., Int. Ed.* **2014**, *53*, 5832−5836.
(30) Denysenko, D.; Werner, T.; Grzywa, M.; Puls, A.; Hagen, V.; Eickerling, G.; Jelic, J.; Reuter, K.; Volkmer, D. Reversible Gas-Phase Redox Processes Catalyzed by Co-Exchanged MFU-4*l*(arge). *Chem. Commun.* **2012**, *48*, 1236−1238.
(31) Brozek, C. K.; Bellarosa, L.; Soejima, T.; Clark, T. V.; Lõpez, N.; Dincă, M. Solvent-Dependent Cation Exchange in Metal−Organic Frameworks. *Chem. - Eur. J.* **2014**, *20*, 6871−6874.
(32) Comito, R. J.; Fritzsching, K. J.; Sundell, B. J.; Schmidt-Rohr, K.; Dincă, M. Single-Site Heterogeneous Catalysts for Olefin Polymerization Enabled by Cation Exchange in a Metal−Organic Framework. *J. Am. Chem. Soc.* **2016**, *138*, 10232−10237.
(33) Dubey, R. J. C.; Comito, R. J.; Wu, Z.; Zhang, G.; Rieth, A. J.; Hendon, C. H.; Miller, J. T.; Dincă, M. Highly Stereoselective Heterogeneous Diene Polymerization by Co-MFU-4*l*: A Single-Site Catalyst Prepared by Cation Exchange. *J. Am. Chem. Soc.* **2017**, *139*, 12664−12669.
(34) Comito, R.; Wu, Z.; Zhang, G.; Lawrence, J.; Korzyński, M.; Kehl, J. A.; Miller, J.; Dincă, M. Stabilized Vanadium Catalyst for Olefin Polymerization by Site Isolation in a Metal−Organic Framework. *Angew. Chem., Int. Ed.* **2018**, *57*, 8135.

https://dx.doi.org/10.1021/acscatal.9b03282
ACS Catal. 2020, 10, 3864−3870

(35) Rojas, R.; Valderrama, M.; Wu, G. Synthesis, Structural Characterization and Ethylene Polymerization Behavior of Complex $[Ph_4P][CrCl_3\{HB(pz)_3\}]$ $[HB(pz)_3$ = Hydrotris(1-pyrazolyl)Borate]. *Inorg. Chem. Commun.* **2004**, *7*, 1295−1297.
(36) García-Orozco, I.; Quijada, R.; Vera, K.; Valderrama, M. Tris(pyrazolyl)methane-chromium(III) Complexes as Highly Active Catalysts for Ethylene Polymerization. *J. Mol. Catal. A: Chem.* **2006**, *260*, 70−76.
(37) Comito, R. J.; Metzger, E. D.; Wu, Z.; Zhang, G.; Hendon, C. H.; Miller, J. T.; Dincă, M. Selective Dimerization of Propylene with Ni-MFU-4*l*. *Organometallics* **2017**, *36*, 1681−1683.
(38) Álvarez, R. P.; Markowicz, A.; Wegrzynek, D.; Cano, E. C.; Bamford, S. A.; Torres, D. H. Quality Management and Method Validation in EDXRF Analysis. *X-Ray Spectrom.* **2007**, *36*, 27−34.
(39) Our DFT model treats **1**·DMF as having three nitrogen, two chlorine, and one oxygen atoms in the primary coordination sphere of chromium as a result of DMF coordination. However, it is very difficult to distinguish nitrogen and oxygen scattering points by our EXAFS method, and therefore, we treated these elements as the same for the sake of simplicity. A reasonably good fit is still obtained despite this assumption.
(40) Kersten, J. L.; Kucharczyk, R. R.; Yap, G. P. A.; Rheingold, A. L.; Theopold, K. H. $[(Tp^{(tBu,Me)})CrR]$: A New Class of Mononuclear, Coordinatively Unsaturated Chromium(II) Alkyls with *cis*-Divacant Octahedral Structure. *Chem. - Eur. J.* **1997**, *3*, 1668−1674.
(41) Camacho-Bunquin, J.; Siladke, N. A.; Zhang, G.; Niklas, J.; Poluektov, O. G.; Nguyen, S. T.; Miller, J. T.; Hock, A. S. Synthesis and Catalytic Hydrogenation Reactivity of a Chromium Catecholate Porous Organic Polymer. *Organometallics* **2015**, *34*, 947−952.
(42) Getsoian, A.; Das, U.; Camacho-Bunquin, J.; Zhang, G.; Gallagher, J. R.; Hu, B.; Cheah, S.; Schaidle, J. A.; Ruddy, D. A.; Hensley, J. E.; Krause, T. R.; Curtiss, L. A.; Miller, J. T.; Hock, A. S. Organometallic Model Complexes Elucidate the Active Gallium Species in Alkane Dehydrogenation Catalysts Based on Ligand Effects in Ga K-Edge XANES. *Catal. Sci. Technol.* **2016**, *6*, 6339−6353.
(43) Zhang, G.; Li, J.; Deng, Y.; Miller, J. T.; Kropf, A. J.; Bunel, E. E.; Lei, A. Structure-Kinetic Relationship Study of Organozinc Reagents. *Chem. Commun.* **2014**, *50*, 8709−8711.
(44) Peacock, A. J. *Handbook of Polyethylene: Structure, Properties, and Applications*; Marcel Dekker, Inc.: New York, 2000.
(45) Guo, L.; Dai, S.; Sui, X.; Chen, C. Palladium and Nickel Catalyzed Chain Walking Olefin Polymerization and Copolymerization. *ACS Catal.* **2016**, *6*, 428−441.
(46) Guan, Z.; Cotts, P. M.; McCord, E. F.; McLain, S. J. Chain Walking: A New Strategy to Control Polymer Topology. *Science* **1999**, *283*, 2059−2062.
(47) Nagel, E. J.; Kirillov, V. A.; Ray, W. H. Prediction of Molecular Weight Distributions for High-Density Polyolefins. *Ind. Eng. Chem. Prod. Res. Dev.* **1980**, *19*, 372−379.
(48) Bhagwat, M. S.; Bhagwat, S. S.; Sharma, M. M. Mathematical Modeling of the Slurry Polymerization of Ethylene: Gas-Liquid Mass Transfer Limitations. *Ind. Eng. Chem. Res.* **1994**, *33*, 2322−2330.
(49) Klet, R. C.; Tussupbayev, S.; Borycz, J.; Gallagher, J. R.; Stalzer, M. M.; Miller, J. T.; Gagliardi, L.; Hupp, J. T.; Marks, T. J.; Cramer, C. J.; Delferro, M.; Farha, O. K. Single-Site Organozirconium Catalyst Embedded in a Metal−Organic Framework. *J. Am. Chem. Soc.* **2015**, *137*, 15680−15683.
(50) Agirrezabal-Telleria, I.; Luz, I.; Ortuño, M. A.; Oregui-Bengoechea, M.; Gandarias, I.; López, N.; Lail, M. A.; Soukri, M. Gas Reactions Under Intrapore Condensation Regime within Tailored Metal−organic Framework Catalysts. *Nat. Commun.* **2019**, *10*, 2076−2083.
(51) Agirrezabal-Telleria, I.; Iglesia, E. Stabilization of Active, Selective, and Regenerable Ni-based Dimerization Catalysts by Condensation of Ethene within Ordered Mesopores. *J. Catal.* **2017**, *352*, 505−514.
(52) Metzger, E. D.; Comito, R. J.; Wu, Z.; Zhang, G.; Dubey, R. C.; Xu, W.; Miller, J. T.; Dincă, M. Highly Selective Heterogeneous Ethylene Dimerization with a Scalable and Chemically Robust MOF Catalyst. *ACS Sustainable Chem. Eng.* **2019**, *7*, 6654−6661.

https://dx.doi.org/10.1021/acscatal.9b03282
ACS Catal. 2020, 10, 3864−3870